EPSC Abstracts
Vol. 8, EPSC2013-840-1, 2013
European Planetary Science Congress 2013

Enceladus Heat Flow from High Spatial Resolution Thermal Emission Observations

J. R. Spencer (1), C. J. A. Howett (1), A. Verbiscer (2), T. A. Hurford (3), M. Segura (3), D. C. Spencer (4)
(1) Southwest Research Institute, USA (spencer@boulder.swri.edu), (2) University of Virginia, USA, (3) Goddard Spaceflight Center, USA, (4) Kenilworth School, UK

Abstract

We estimate the total power radiated from Enceladus' tiger stripes, using Cassini CIRS observations with spatial resolution high enough to separate the active tiger stripe emission from the background. The resulting radiated power, 4.2 GW (to which should be added 0.5 GW of plume latent heat and possible inter-stripe emission), is lower than previous estimates based on the integrated south polar emission, though still higher than expected from steady-state tidal heating.

1. Introduction

The magnitude of Enceladus' tidal heat flow is a fundamental constraint on dissipation mechanisms, the orbital and thermal evolution of Enceladus, and the mechanisms that generate the plumes [1, 2]. The south polar tidal heat flow can be constrained directly from the observed thermal emission from the south pole, after subtraction of estimated passive emission due to re-radiated absorbed sunlight. The Cassini Composite Infrared Spectrometer (CIRS) observes this emission using a single 10 – 600 cm^{-1} detector ("FP1") with 4 mrad spatial resolution, and two 1x10 arrays covering 600 – 1100 cm^{-1} ("FP3") and 1100 – 1500 cm^{-1} ("FP4"), both with 0.29 mrad spatial resolution. Most of both the endogenic and passive emission is radiated at FP1 wavenumbers, where CIRS spatial resolution is relatively low.

FP3 observations in 2005 of the integrated south polar emission, extrapolated to lower wavenumbers by fitting a graybody spectrum to the FP3 spectrum and correcting for estimated passive emission, gave an estimated heat flow of 5.8 ± 1.9 GW [3]. Higher resolution FP3 observations in 2008 showed that thermal emission is concentrated along the length of all four tiger stripes ([4], Fig. 1). FP1 observations in 2008 of the integrated south polar emission, again after subtraction of estimated passive emission, gave a higher heat flow estimate of 15.8 ± 3.1 GW [4], with the increase attributed to the presence of a low-temperature component radiating at FP1 wavelengths but not significantly at FP3 wavelengths.

2. New Analysis

The previous heat flow estimates were based on observations that did not resolve the tiger stripes from their surroundings, so passive emission from the surroundings had to be modeled and subtracted to determine endogenic heat. Here we use higher spatial resolution observations to spatially separate the tiger stripe emission, which must be endogenic, from background emission which is expected to be partly or entirely passive.

We model the surfaces radiating the endogenic emission as continuous ribbons of material of temperature $T(l)$ and width $W(l)$ which vary smoothly with distance l along the tiger stripes and associated warm fractures. T and W are adjusted to match the spatial and wavelength dependence of the emission seen in specific CIRS observations, using a forward model.

The most extensive FP3 map of the tiger stripes, obtained on orbit 61 in March 2008 (Fig. 1), can be matched with a single relatively high temperature endogenic component, denoted by subscript H, with $T_H(l)$ varying spatially between 120 and 165 K, and $W_H(l)$ varying between 60 and 330 meters. The best spatially resolved constraint on lower-wavenumber emission, an FP1 scan across the tiger stripes Damascus, Baghdad, and Cairo from orbit 136 in August 2010 (Fig. 1) shows that an additional lower temperature component is also needed (Fig. 2). However the limited spatial coverage of this and other FP1 scans does not allow unique constraints on the spatial distribution of the low temperature component. To estimate the contribution of this component (denoted by subscript L), we constrain T_L and W_L from the wavelength-dependent FP1 signature where the Rev 136 scan crosses the tiger

stripes (Fig. 2), and extrapolate to the rest of the system by assuming that both T_L and W_L/W_H are independent of location. We then re-fit all parameters using these assumptions.

The resulting total heat flow is 2.7 GW and 1.5 GW from the high and low temperature components respectively, for a total of 4.2 GW. Enceladus' power output also includes the latent heat of the escaping plume (~0.5 GW [2]), giving a total output of ~4.7 GW. There may be additional endogenic heat from the regions between the tiger stripes, included in previous estimates but excluded here, which may account for some of the discrepancy with earlier estimates. It is also possible that previous models under-estimated the passive contribution to the integrated south polar emission (for instance due to spatial variability of thermophysical properties), and thus over-estimated of the endogenic component.

The inconsistency of heat flows derived from different techniques highlights the difficulty of these measurements, indicating that all heat flow estimates should be treated with caution. However all estimates are much larger than the expected maximum steady-state tidal heating of 1.1 GW [5].

Acknowledgements

The work was funded by Cassini and NASA Outer Planets Research program grant NNX11AM47G

References

[1] Spencer, J., and Nimmo, F.: Enceladus: An active ice world in the Saturn system Ann. Rev. Earth Planet. Sci. 41, 26.1–26.25, 2013.

[2] Ingersoll, A., and Pankine, A.: Subsurface heat transfer to Enceladus: conditions under which melting occurs. Icarus 20, 594, 2010.

[3] Spencer J, et al.: Cassini encounters Enceladus: background and the discovery of a south polar hot spot. Science 311 1401, 2006.

[4] Howett C, Spencer J, Pearl J, Segura M.: High heat flow from Enceladus' south polar region measured using 10–600 cm^{-1} Cassini/CIRS data. J. Geophys. Res. 116, E03003, 2011.

[5] Meyer J, and Wisdom J.: Tidal heating in Enceladus. Icarus 188, 535, 2007.

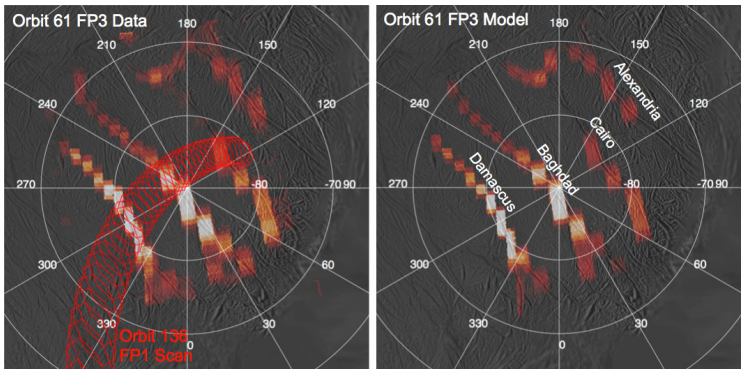

Figure 1: Constraining the tiger stripe emission distribution model using the orbit 61 CIRS FP3 scan of the tiger stripe system. The left panel shows observed 600 – 850 cm^{-1} radiance, the right panel shows the simulated observation derived from the best-fit model. The left panel also shows (red) the location of the orbit 136 FP1 scan used to constrain the longer-wavelength emission from the tiger stripes (Fig. 2).

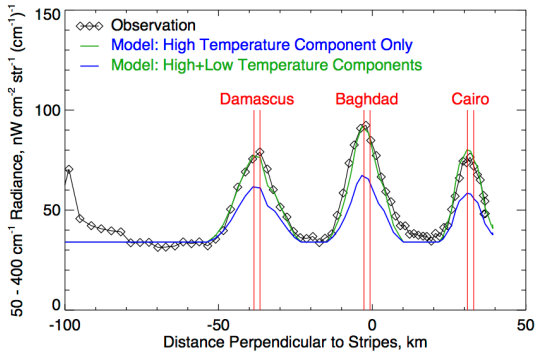

Figure 2: Profile of low-wavenumber FP1 radiation across three of the tiger stripes (Fig. 1) from orbit 136, compared to predictions from our best-fit model of tiger stripe temperatures, with and without the inclusion of a low-temperature component. The model also includes a constant background radiance, assumed here to be passive re-radiated sunlight. This FP1 scan reveals that the high-temperature component fitted to the FP3 observations (Fig. 1) does not account for all the radiated power at low wavenumbers, and an additional low-temperature component is need to match the data.